Bioorganic & Medicinal Chemistry 16 (2008) 9283–9294

Contents lists available at ScienceDirect

Bioorganic & Medicinal Chemistry

journal homepage: www.elsevier.com/locate/bmc

The molecular interactions of buspirone analogues with the serotonin transporter

Małgorzata Jarończyk [a], Zdzisław Chilmonczyk [a], Aleksander P. Mazurek [a], Gabriel Nowak [b], Aina W. Ravna [c], Kurt Kristiansen [c], Ingebrigt Sylte [c,*]

[a] National Medicines Institute, 30/34 Chełmska Street, 00-725 Warsaw, Poland
[b] Institute of Pharmacology PAS, 12 Smętna Street, 31-343 Cracow, Poland
[c] Department of Pharmacology, Institute of Medical Biology, University of Tromsø, N-9035 Tromsø, Norway

ARTICLE INFO

Article history:
Received 16 April 2008
Revised 26 August 2008
Accepted 2 September 2008
Available online 5 September 2008

Keywords:
Serotonin transporter
Serotonin reuptake inhibitors
Docking
Molecular modelling

ABSTRACT

A major problem with the selective serotonin reuptake inhibitors (SSRIs) is the delayed onset of action. A reason for that may be that the initial SSRI-induced increase in serotonin levels activates somatodendritic 5-HT_{1A} autoreceptors, causing a decrease in serotonin release in major forebrain areas. It has been suggested that compounds combining inhibition of the serotonin transport protein with antagonistic effects on the 5-HT_{1A} receptor will shorten the onset time. The anxiolytic drug buspirone is known as 5-HT_{1A} partial agonist. In the present work, we are studying the inhibition of the serotonin transporter protein by a series of buspirone analogues by molecular modelling and by experimental affinity measurements. Models of the transporter protein were constructed using the crystal structure of the *Escherichia coli* major facilitator family transporter-LacY and the X-ray structure of the neurotransmitter symporter family (NSS) transporter-$LeuT_{Aa}$ as templates. The buspirone analogues were docked into both SERT models and the interactions with amino acids within the protein were analyzed. Two putative binding sites were identified on the $LeuT_{Aa}$ based model, one suggested to be a high-affinity site, and the other suggested to be a low-affinity binding site. Molecular dynamic simulations of the LacY based model in complex with ligands did not induce a helical architecture of the LacY based model into an arrangement more similar to that of the $LeuT_{Aa}$ based model.

1. Introduction

Selective serotonin reuptake inhibitors (SSRIs) are today the most widely used agents in the treatment of depression and several other neuropsychiatric and related disorders.[1] SSRIs increase the concentration of serotonin at the synapses by inhibiting the neuronal reuptake of serotonin, and thus enhance serotonergic neuronal transmission. The molecular target of SSRIs is the serotonin transporter protein (SERT), responsible for the transport of serotonin back into the pre-synaptic cell.

A major problem with the SSRIs is the delayed onset of action.[2,3] It is suggested that the initial SSRI-induced increased level of serotonin in the vicinity of the serotonergic cell bodies activates somatodendritic 5-HT_{1A} autoreceptors, causing a decrease in serotonin release in major forebrain areas.[1] This negative feedback limits the increment of synaptic serotonin that can be induced by SSRIs. Animal models have indicated that antagonizing the 5-HT_{1A} autoreceptor limits the negative feedback control.[4] A combination therapy aiming to inhibit SERT and antagonize the 5-HT_{1A} autoreceptors is therefore expected to shorten the onset time of SSRIs.[5,6] Thus, the concept of developing dual-acting agents antagonizing the 5-HT_{1A} pre-synaptic autoreceptors and inhibiting SERT (5-HT_{1A}/SSRI) has emerged.[7–9]

Despite clinical significance, very little is known about the detailed three dimensional (3D) structure of SERT, and how the 3D structure is related to function and ligand recognition. SERT is a secondary transporter and belongs to the family of Na^+/Cl^- dependent neurotransmitter transporters (NSS). This family also includes transporters for dopamine (DAT), norepinephrine (NET), glycine (GlyT) and γ-aminobutyric acid (GABA).[10] Secondary transporters use the energy from a concentration gradient previously established by a primary active transport process to transport a molecule of interest against its concentration gradient.

The largest family of secondary transporters is the major facilitator superfamily (MSF). The 3D structures of three *Escherichia coli*

Abbreviations: MD, molecular dynamics; MM, molecular mechanics; RESP, restrained electrostatic potentials; SSRI, selective serotonin reuptake inhibitors; TMH, transmembrane helix; SERT, 5-HTT, serotonin transporter; 5-HT, serotonin; ICM, internal coordinate mechanics; RMS, root mean square; RMSD, root mean square deviation.

* Corresponding author. Tel.: +47 77 644 705; fax: +47 77 645 310.
E-mail address: sylte@fagmed.uit.no (I. Sylte).

0968-0896/$ - see front matter © 2008 Elsevier Ltd. All rights reserved.
doi:10.1016/j.bmc.2008.09.005

transporter proteins of the MSF family have been determined by X-ray crystallography at atomic resolution: EmrD,[11] GlpT[12] and LacY.[13] These structures indicate that MSF proteins with 12 transmembrane α-helices (TMHs) share a common architecture of the membrane spanning region, organized in symmetrical N- and C-terminal domains, each of six TMHs, with overall structural topologies resembling each other. In 2005 the crystal structure of bacterial homologue of Na^+/Cl^--dependent transporters from *Aquifex aeolicus* ($LeuT_{Aa}$), was solved at 1.65 Å with the substrate leucine, and Na^+ ions bound.[14] The X-ray structure indicated that this family has 12 TMHs, but the helical packing seems different from that of the MSF family.

We have previously constructed 3D models of SERT, DAT and NET using the X-ray structure of LacY from *E. coli* as a template.[15] The $LeuT_{Aa}$ structure is so far the X-ray crystal structure with the highest similarity to human monoamine transporters, both in sequence (overall ~20%) (Fig. 1) and function, and is believed to offer an opportunity to build more reliable models of monoamine transporters. Thus, we updated the SERT model using the X-ray structure of $LeuT_{Aa}$ as template.[16]

Following binding of extracellular substrates and electrolytes to an 'outward-facing' conformation, the transporter alternates to an 'inward-facing' conformation powered by the inwardly directed electrochemical potential for ions. Upon release of the substances

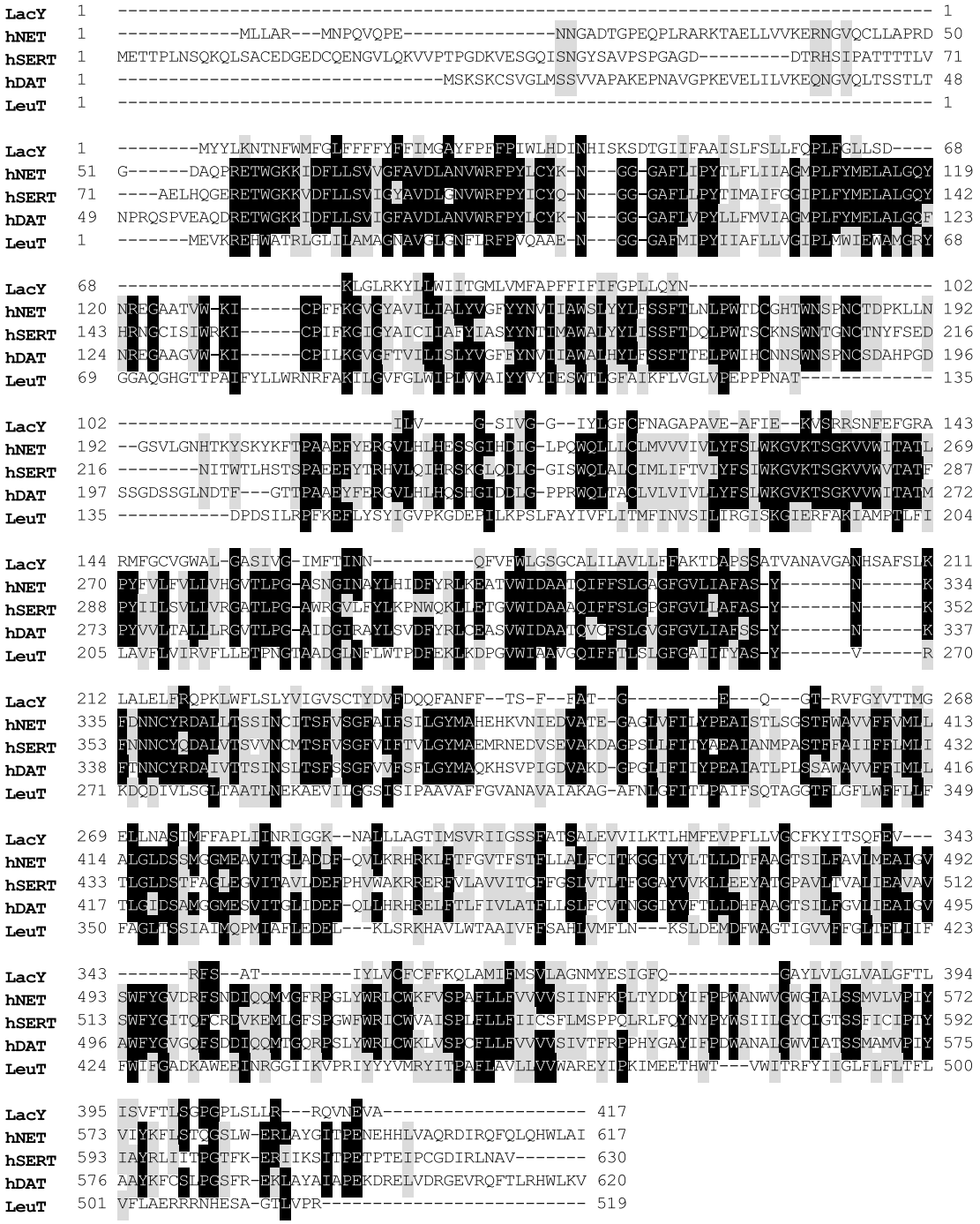

Figure 1. Amino acid sequence alignments of LacY, human norepinephrine (hNET), human serotonin (hSERT), human dopamine (hDAT) and the $LeuT_{Aa}$ transporters. The alignment has been generated using Bioedit.

to the cytosol, the transporter reorients to the 'outward-facing' conformation. In this process, several transporter domains are thought to undergo large-scale conformational changes. Therefore, SERT needs to have a very flexible 3D folding, and the conformation recognized by a substrate may therefore not be completely similar to that of models constructed directly from X-ray structure templates. Although the X-ray structures of LacY and $LeuT_{Aa}$ indicate that it is less likely that the helical architecture of $LeuT_{Aa}$ can be converted into a helical architecture more similar to that of LacY, it cannot be entirely ruled out that the helical architecture observed in these structures represent different energetically favourable conformations of the same folding class.

In the present study, two models of SERT were constructed. One model was constructed using the X-ray structure of LacY solved at 3.5 Å[13] as template. LacY structure represents an inward-facing conformation, as evidenced by a large internal hydrophilic cavity open to the cytoplasmic side. The second model was constructed using the X-ray crystal structure of $LeuT_{Aa}$ as template. The $LeuT_{Aa}$ structure represents a conformation in which the substrate leucine and two sodium ions are occluded from solution both on the periplasmic and cytoplasmic side.

Both SERT models were used to study the interactions with a series of buspirone analogues with dual SERT/5-HT_{1A} activity. The binding affinity for SERT was experimentally determined (Table 1), whilst the binding affinities for the 5-HT_{1A} receptor have been reported previously.[17–19] Molecular dynamics simulations with the LacY based model were also performed in order to study if the helical architecture could be changed into an arrangement more similar to that of $LeuT_{Aa}$ during simulation.

Table 1
Molecular structure and affinities of the buspirone analogues

Compound	Structure	Inhibition constant [^{3}H]5-HT IC_{50}, nM
1	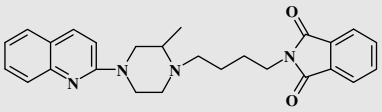	33 8*
2	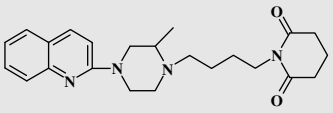	50*
3	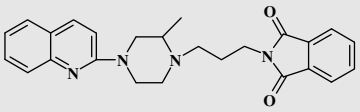	80*
4	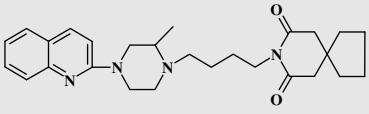	75
5	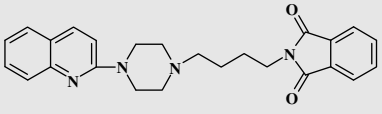	95
6	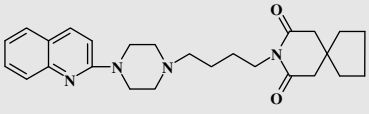	112
7	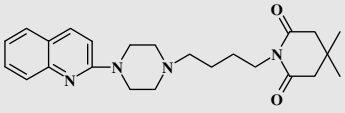	146

The inhibition constants (IC_{50}) is given in nM.
* The inhibition constant of [^{3}H]5-HT at human tissue.

2. Results

2.1. SERT models

The LacY based model indicated that amino acids lining the central cavity consisting of TMH1, TMH2, TMH3, TMH4, TMH5, TMH7, TMH8, TMH10 and TMH11 were in close proximity to a putative substrate-binding area (Fig. 6A and Table 2). The $LeuT_{Aa}$ based model indicated that amino acids within TMH1, TMH3, TMH6, TMH8 and TMH10 may line the substrate-binding area (Fig. 6B and Table 3). In spite of different templates, there are several similarities in the binding site architecture between the two models, and TMH1 and TMH3 are lining a putative-binding pocket in both models (Fig. 6). The ICM PocketFinder also identified a possible low-affinity binding site on the $LeuT_{Aa}$ based model consisting of amino acids in TMH1, TMH6, TMH10 and TMH11 (Figs. 3, 8 and Table 4).

MD simulations were performed for complexes of the LacY based SERT model with buspirone analogues. These MDs were performed in order to study the interactions with buspirone analogues and if the helical architecture could change into a more similar to that of the $LeuT_{Aa}$ based SERT model. Large RMSD for TMH2, TMH3, TMH4, TMH7, TMH8 and TMH11 were observed between the energy minimized structure before MD and the energy minimized average structure after MD without a ligand (Table 5). The RMSD of TMH1 between the average structures after MD without and with ligands was large for all ligands (in the range of 0.87–1.23) (Table 5). The RMSD of TMH3 between the average structures after MD without and with ligands (1)–(4) were large (Table 5), indicating that these ligands with quite high SERT affinity (Table 1) induced large structural displacements into TMH3 of the LacY based SERT model. Table 5 also indicates that ligand (**2**) induced large displacements into TMH8, while ligand (4) induced large displacements of TMH2. For ligands (**5**)–(**7**) quite large displacements were introduced into TMH2 and TMH7.

Figure. 7 shows the electrostatic distribution of the SERT models calculated by the Rebel module of the ICM program.[20] The loops and terminals were not included in the SERT models. The calculations of the electrostatic potentials indicated that the SERT is mainly negatively charged in the area of the substrate translocation pocket. The distribution of electrostatic potentials also indicated that extracellular parts are mainly negative charged, while the intracellular parts are mainly positively charged.

2.2. The ligand–transporter interactions

The buspirone analogues interacted with the outward-facing LacY based SERT model in a pore formed between TMHs 1, 2, 4, 5, 7, 8, 10, 11 (Table 2). Calculations indicated that the ligands bound to the LacY based model with interaction energies in the range of −13.1 to −18.3 kcal/mol. Ligand (**4**) had the strongest interaction energy with the LacY based SERT model. All ligands interacted with Tyr95 (TMH1); Trp271 (TMH4); Tyr289 (TMH5); Leu383 (TMH7) and Phe422 (TMH8) in the binding site. Additionally, all ligands except compound (**3**) interacted with Asp98, Val102 in TMH1 and Tyr267 in TMH4. In contrast to the others, compounds (**2**) and (**5**) did not interact with Leu99 in TMH1. Compounds (**1**), (**2**), (**4**), (**6**) and (**7**) interacted with Asn101 and Phe105 in TMH1, and Phe117 in TMH2. In contrast to other ligands compound (**4**) did not have van der Waals contacts with Trp282 in

Table 2
Amino acid residues of the LacY based SERT model having van der Waals contacts with the ligands after docking

Ligand	Transporter domain	Amino acid residue
1	TMH 1	Tyr95, Asp98, Leu99, Asn101, Val102, Phe105, Pro106
	TMH 2	Phe117, Pro120, Leu123, Met124, Phe127, Gly128, Pro131, Leu132
	TMH 4	Leu257, Met260, Phe263, Thr264, Tyr267, Phe268, Trp271
	TMH 5	Trp282, Tyr289
	TMH 7	Phe380, Leu383
	TMH 8	Phe422
	TMH 10	Val512, Tyr516
	TMH 11	Phe548, Ile552, Phe556
2	TMH 1	Tyr95, Asp98, Asn101, Val102, Trp103, Phe105, Pro106, Tyr107
	TMH 2	Phe117, Tyr121, Met124
	TMH 4	Trp253, Leu257, Met260, Tyr267, Trp271
	TMH 5	Trp282, Thr286, Tyr289
	TMH 7	Phe380, Leu383, Gly384, Ala387, Glu388, Met389
	TMH 8	Thr409, Glu412, Asn416, Ala418, Ser419, Phe422, Ala423
	TMH 10	Ala509
3	TMH 1	Val92, Tyr95, Leu99
	TMH 4	Trp271
	TMH 5	Val281, Trp282, Ala285, Thr286, Tyr289
	TMH 7	Phe380, Val382, Leu383, Gly384, Met386, Ala387
	TMH 8	Glu412, Asn416, Ala415, Ala418, Ser419, Phe422
	TMH 10	Ala505, Glu508, Ala509, Val512, Tyr516
	TMH 11	Phe548
4	TMH 1	Tyr95, Asp98, Leu99, Asn101, Val102, Phe105
	TMH 2	Ala116, Phe117, Pro120, Tyr121
	TMH 4	Met260, Phe263, Thr264, Tyr267, Phe268, Trp271
	TMH 5	Tyr289
	TMH 7	Phe380, Leu383, Gly384, Met386, Ala387
	TMH 8	Asn416, Ser419, Phe422
	TMH 10	Ala509, Val512
	TMH 11	Phe556
5	TMH 1	Tyr95, Asp98, Val102, Pro106
	TMH 4	Tyr267, Trp271
	TMH 5	Trp282, Thr286, Tyr289
	TMH 7	Phe380, Leu383, Met386, Ala387
	TMH 8	Glu412, Asn416, Ala415, Ala418, Ser419, Phe422
	TMH 10	Ala505, Leu506, Glu508, Ala509, Val512, Tyr516
	TMH 11	Ile552
6	TMH 1	Tyr95, Asp98, Leu99, Asn101, Val102, Phe105
	TMH 2	Phe117, Pro120, Tyr121, Met124
	TMH 4	Ala256, Leu257, Cys258, Met260, Leu261, Phe263, Thr264, Tyr267, Phe268, Trp271
	TMH 5	Trp282, Tyr289
	TMH 7	Ile379, Val382, Leu383, Met386, Ala387
	TMH 8	Glu412, Asn416, Ala418, Ser419, Phe422
	TMH 10	Ala505, Glu508, Ala509, Val512, Leu506
7	TMH 1	Tyr95, Asp98, Leu99, Asn101, Val102, Trp103, Phe105, Pro106
	TMH 2	Ala116, Phe117
	TMH 4	Tyr267, Trp271
	TMH 5	Trp282, Ala285, Thr286, Tyr289
	TMH 7	Leu383, Met386, Ala387, Glu388, Met389
	TMH 8	Thr409, Glu412, Asn416, Ala418, Ser419, Thr420, Phe422, Ala423,
	TMH10	Ala509, Val512

Table 3
Amino acid residues of the $LeuT_{Aa}$ based SERT model having van der Waals contacts with the ligands after docking into the putative high-affinity binding site

Ligand	Transporter domain	Amino acid residue
1	TMH 1	Ala96, Tyr95, Asp98, Leu99, Gly100, Asn101, Trp103, Arg104
	TMH 3	Ala169, Phe170, Ile172, Ala173, Tyr175, Tyr176
	TMH 6	Phe335, Ser336, Leu337, Gly338, Pro339, Phe341, Val343
	TMH 8	Ser438, Thr439, Ala441, Gly442, Leu443
	TMH10	Glu493, Thr497
2	TMH 1	Ala96, Tyr95, Asp98, Leu99, Gly100, Trp103, Arg104
	TMH 3	Ile168, Ala169, Ile172, Ala173, Tyr175, Tyr176, Asn177, Ile179
	TMH 6	Phe334, Phe335, Ser336, Leu337, Gly338, Phe341
	TMH 8	Ser438, Thr439, Ala441, Gly442, Leu443
	TMH10	Thr497
3	TMH 1	Ala96, Tyr95, Asp98, Leu99, Gly100, Trp103, Arg104
	TMH 3	Ile168, Ala169, Phe170, Ile172, Ala173, Tyr175, Tyr176, Asn177, Ile179
	TMH 6	Phe334, Phe335, Leu337, Gly338, Phe341, Val343
	TMH 8	Ser438, Thr439, Ala441, Gly442
	TMH10	Glu493, Thr497
4	TMH 1	Ala96, Tyr95, Asp98, Leu99, Gly100, Asn101, Trp103, Arg104
	TMH 3	Ile168, Ala169, Phe170, Ile172, Ala173, Tyr175, Tyr176, Asn177, Ile179
	TMH 6	Gln332, Phe334, Phe335, Ser336, Leu337, Gly338, Pro339, Phe341
	TMH 8	Ser438, Thr439, Gly442, Leu443
	TMH10	Glu493, Thr497
5	TMH 1	Ala96, Tyr95, Asp98, Leu99, Gly100, Trp103, Arg104
	TMH 3	Ile168, Ala169, Ala173, Tyr175, Tyr176, Asn177, Ile179
	TMH 6	Phe335, Ser336, Leu337, Gly338, Phe341, Val343,
	TMH 8	Ser438, Thr439, Ala441, Gly442,
	TMH10	Thr497
6	TMH 1	Ala96, Tyr95, Asp98, Gly100, Asn101, Trp103, Arg104
	TMH 3	Ile168, Ala169, Phe170, Ile172, Ala173, Tyr176, Asn177, Ile179
	TMH 6	Gln332, Phe335, Ser336, Leu337, Gly338, Phe341, Val343
	TMH 8	Ser438, Thr439, Phe440, Ala441, Gly442, Leu443
	TMH10	Thr497
7	TMH 1	Ala96, Tyr95, Asp98, Leu99, Gly100, Trp103, Arg104
	TMH 3	Ile168, Ala169, Ile172, Ala173, Tyr175, Tyr176, Asn177
	TMH 6	Phe334, Phe335, Ser336, Leu337, Gly338, Phe341, Val343,
	TMH 8	Ser438, Thr439, Phe440, Ala441, Gly442, Leu443
	TMH10	Glu493, Thr497

TMH5. Compounds (**3**)–(**7**) interacted with Met386 in TMH7, and similar to compound (**2**) they also interacted with Ala387. The compounds (**2**)–(**7**) interacted with amino acids: Glu412, Asn416, Ala418 and Ser419 in TMH8 and Ala509 in TMH10.

In the SERT model based on the $LeuT_{Aa}$ crystal structure the compounds interacted in the pore formed between TMHs 1, 3, 6, 8 and 10 (Table 3). Calculations indicated that the ligands bound to the $LeuT_{Aa}$ based model with interaction energies in the range of −12.6 to −23.3 kcal/mol. As for the LacY based model, ligand (**4**) had the strongest interaction energy with the model. Residues participating in ligand binding were: Tyr95, Ala96, Asp98, Gly100, Trp103 and Arg104 (TMH1); Ala169, Ile172, Ala173, Tyr176 (TMH3); Phe335, Ser336, Leu337, Gly338, Phe341 (TMH6); Ser438, Thr439, Gly442 (TMH8) and Thr497 (TMH10). Compound (**1**), (**4**) and (**6**) interacted with Asn101 in TMH1. All the compounds except (**1**) interacted with Ile168 in TMH3. In addition ligands (**1**), (**3**), (**4**), (**7**) interacted with Glu493 in TMH10.

The ICMPocketFinder also identified a putative-binding site constituting amino acids in TMHs: 1, 6, 10 and 11 (Table 4). The calculations showed that the ligands interacted with this binding site with interaction energies in the range of −6.2 to −9.2 kcal/mol, with ligand (**5**) as the strongest binder. This binding site may correspond to a possible low-affinity binding site. Residues involved in ligand binding in this region were: Arg104, Tyr107 in TMH1; Ile327, Asp328, Ala331 in TMH6; Lys490 in TMH10. In addition, all the ligands except compound (**2**) interacted with Pro560 in TMH11, while only compound (**4**) and (**5**) did not have van der Waals contacts with Phe556. Compound (**3**) in contrast to the others did not interact with Ile108 and Gln111 in TMH1. All compounds except of compound (**2**) interacted with Thr323 and

Table 4
Amino acid residues of the $LeuT_{Aa}$ based SERT model having van der Waals contacts with the ligands after docking into the putative low-affinity binding site

Ligand	Transporter domain	Amino acid residue
1	TMH 1	Arg104, Tyr107, Ile108, Gln111
	TMH 6	Gln322, Thr323, Gly324, Val325, Ile327, Asp328, Ala331
	TMH 10	Glu493, Glu494, Gly498,
	TMH 11	Phe556, Pro560
2	TMH 1	Arg104, Tyr107, Ile108, Gln111
	TMH 6	Ile327, Asp328, Ala331
	TMH 10	Lys490, Glu493, Glu494, Gly498
	TMH 11	Phe556
3	TMH 1	Arg104, Tyr107
	TMH 6	Thr323, Gly324, Ile327, Asp328, Ala331
	TMH 10	Lys490, Glu493, Glu494, Gly498, Pro499
	TMH 11	Phe556, Pro560, Arg564
4	TMH 1	Arg104, Tyr107, Ile108, Gln111
	TMH 6	Gln322, Thr323, Gly324, Val325, Ile327, Asp328, Ala331
	TMH 10	Lys490, Glu493, Glu494, Gly498, Pro499
	TMH 11	Pro560
5	TMH 1	Arg104, Tyr107, Ile108, Gln111
	TMH 6	Gln322, Thr323, Gly324, Val325, Ile327, Asp328, Ala331
	TMH 10	Lys490, Glu493
	TMH 11	Pro560
6	TMH 1	Arg104, Tyr107, Ile108, Gln111
	TMH 6	Gln322, Thr323, Gly324, Val325, Ile327, Asp328, Ala331
	TMH 10	Lys490, Glu493, Glu494, Gly498,
	TMH 11	Phe556, Pro560
7	TMH 1	Arg104, Tyr107, Ile108, Gln111
	TMH 6	Gln322, Thr323, Gly324, Val325, Ile327, Asp328, Ala331
	TMH 10	Lys490, Glu493, Glu494, Gly498,
	TMH 11	Phe556, Pro560

Table 5
RMSD of TMHs (backbone atoms) between the average energy minimized SERT conformations

TMH domains of SERT	RMSD before and after MD without ligand	RMSD of TMHs after MD with and without ligand Ligand						
		1	**2**	**3**	**4**	**5**	**6**	**7**
TMH 1	1.05	0.87	1.11	1.23	1.00	0.89	1.07	1.08
TMH 2	1.88	1.04	0.56	0.74	1.32	1.04	0.81	1.63
TMH 3	1.94	1.25	1.39	1.19	1.18	0.75	0.63	0.89
TMH 4	2.01	1.14	0.61	0.83	0.62	0.67	0.71	0.45
TMH 5	0.91	0.51	0.75	0.65	0.52	0.77	0.54	0.62
TMH 6	0.78	0.64	0.41	0.45	0.49	0.73	0.32	0.33
TMH 7	1.31	0.50	0.63	0.33	0.40	1.00	1.05	0.81
TMH 8	2.06	0.73	1.79	0.33	0.86	0.56	0.95	0.72
TMH 9	0.57	0.14	0.72	0.33	0.28	0.20	0.12	0.85
TMH 10	0.99	0.46	0.63	0.57	0.21	0.48	0.59	0.36
TMH 11	1.75	0.66	0.76	0.81	1.15	0.95	0.72	0.94
TMH 12	1.00	0.85	0.76	0.73	0.77	0.29	0.68	0.88

Gly324 in TMH2, while all except of compound (**5**) had close contacts with Glu494 and Gly498 in TMH6. The compounds also interacted with Asp400 and Gly402 located in extracellular loop (EL4) connecting TMH7 and TMH8.

3. Discussion

The SERT models in the present study were based on different 3D structures of bacterial secondary transporter proteins. Both templates have a helical architecture of 12 TMHs, but their helical packing is different. However, the two templates and thereby the models generated may represent different conformational states of the same overall folding. The LacY template may represent the inward-facing conformation, while the $LeuT_{Aa}$ template may represent the substrate-occluded conformation closed at both sides. An outward-facing conformation of the SERT model based on LacY was obtained by rigid-body rotation of the two transmembrane domains (1–6 TMH and 7–12 TMH) relative to each other. The stereochemical quality of the SERT models was checked using the NIH structure analyses and verification server (SAVS) (http://nihserver.mbi.ucla.edu/SAVES_3/). The Ramachandran plot of the $LeuT_{Aa}$ based SERT model indicated that 95.4% of the amino acids residues were in structurally most favoured regions, 4.3% were in additionally allowed regions, 0.3% were in generously allowed regions and 0% in disallowed regions. The corresponding percentages for the $LeuT_{Aa}$ template (PDB code: 2a65) were: 94.5%, 5.5%, 0.0% and 0.0%. The Ramachandran plot of the LacY based SERT model showed that 84.4% were in most favoured regions, 14.7% in additionally allowed regions, 0.7% in generously allowed and 0.2% in disallowed regions. The corresponding percentages for the LacY template (PDB code: 1PV6) were: 79.0%, 19.1%. 1.4% and 0.5%. These results indicate that both models are geometrically acceptable.

The accuracy of a computer model generated by homology depends on sequence and functional similarities between the target and the template. However, it is well known that active sites and membrane spanning regions can have very similar geometries for quite distantly related proteins. Even at an overall sequence similarity less than 15% there may give considerable structural similarities in functional similar regions of membrane proteins. The overall sequence identity between SERT and $LeuT_{Aa}$ is 21%, but up to 50% in some of the membrane spanning helices (Fig. 1), while the sequence identities within the transmembrane regions between LacY and SERT are around 11–13%. Thus, $LeuT_{Aa}$ is closer to SERT both in sequence and function, and should be regarded as a better template for modelling SERT than LacY. The $LeuT_{Aa}$ structure has also been used as a template for three recent models of the SERT apo protein.[21–23] The binding of 5-HT and escitalopram to a $LeuT_{Aa}$ based SERT model was also studied by molecular modelling.[24]

The accuracy of the amino acid sequence alignment between the template and the target is the most important single component for the quality of homology-based model. The alignment in the present study (Fig. 1) was based on alignments from previous studies,[14,15] that were adjusted based on experimental observations, particularly from site-directed mutagenesis experiments. Based on structural and functional similarities and information from site-directed mutagenesis we feel that the alignment (Fig. 1) contributes to a reasonable structural model of SERT based on the $LeuT_{Aa}$ template, while the alignment between SERT and LacY is more uncertain, and thereby also a more uncertain SERT model. Based on experiences from other membrane protein families (like G-protein coupled receptors) indicating that sequences similarities lower than 15% may give similar folds of functionally related regions, we can not rule out that the LacY based SERT model represents another conformational stage of the same folding class.

If the LacY and $LeuT_{Aa}$ X-ray structures represent different conformational stages of same folding class, the $LeuT_{Aa}$ based SERT model should represent a ligand bound conformation of SERT, while the LacY based SERT models represent the outward- and inward-facing conformations. However, the conformation recognized by a ligand/inhibitor and the conformational changes that take place during substrate binding may generate helical architectures different to those observed both in the LacY and the $LeuT_{Aa}$ based SERT models. The conformational changes being necessary

for substrate and ion translocation of the TMHs may involve large conformational changes. If these models represent different low-energy conformations of the same overall folding, the average structures from MD simulations may provide insight into the structural changes of SERT upon ligand binding. The MDs indicated that the largest structural differences induced upon ligand binding were in TMH1, TMH2, TMH3, TMH4, TMH7, TMH8 and TMH11 (Table 5), since RMSD between the initial SERT model and the models after MD with ligands were largest in theses TMHs. The MD also indicated that the compounds (**1**)–(**4**) induced larger conformational changes into TMH3 than did the other compounds, while compounds (**5**)–(**7**) induced largest displacements into TMH7 than did the other compounds. Ligands (**1**)–(**4**) were located closer to Phe380 and Gly384 in TMH7 and interactions between the methyl group at the piperazine ring and Phe380 could influence the stability of the ligand–SERT complex. Thus binding of methylated buspirone analogues near TMH7 could result in large displacements of TMH3 in order to accommodate ligands at the binding site. Compounds (**1**)–(**4**) have stronger SERT affinity than compounds (**5**)–(**7**) (Table 1). Interestingly, compounds (**2**) and (**7**) that are quite similar in structure both induced large displacement into TMH9, while the other did not. Only the ligands (**2**) and (7) interacted with Thr409 and Ala423 in TMH8, thus a movement of TMH9 seems necessary to allow for such interactions.

Calculations of the electrostatic potentials at the surface of both SERT models (Fig. 7), indicated that the region of the predicted translocation pathway is mainly negative for both models. This might indicate that the positively charged substrate 5-HT is directed into the substrate translocation area by electrostatic interactions.

The binding site of the LacY based model consisted of amino acids in TMHs 1, 2, 4, 5, 7, 8, 10 and 11, while the corresponding binding site of the $LeuT_{Aa}$ based model (the high-affinity binding site) constituted amino acids within TMHs 1, 3, 6, 8 and 10. Site-directed mutagenesis data on SERT, DAT and NET showed that amino acids in TMH1 (Tyr95, Asp98, SERT numbering),[57,25–27] TMH3 (Ala169, Ile172, Tyr176, Met180, SERT numbering),[14,25,27–31] TMH6 (Trp310, Ph316, SERT numbering)[32,33] and TMH8 (Ser438, SERT numbering)[32,34] are important for ligand binding. In agreement with site-directed mutagenesis both SERT models included TMH1 and TMH8 in the ligand-binding area (Tables 2–4), but only the $LeuT_{Aa}$ based SERT model suggested that amino acids in TMH3 (including Ala169, Ile172 and Tyr176) and TMH6 were directly involved in ligand binding. In both SERT models the compounds interacted strongly with Asp98 and Tyr95 in TMH1. However, the only exception was compound (**3**) that interacted with few residues of TMH1 of the LacY based model, and not with Asp98. The importance of Tyr95 and Asp98 in TMH1 for ligand binding has been confirmed experimentally.[25,34]

In addition, studies using substituted cysteine accessibility method (SCAM) implicated that Gly100 and Asn101 together with Asp98 and Tyr95 form a critical stripe of amino acids that can be protected from methanethiosulfonate (MTS) inactivation by 5-HT co-incubation.[34] MTS reagents are useful for identifying residues exposed to the external medium, involved in ligand contacts or domains conformationally linked to ligand occupancy in receptors and channels.[45–48] Ligand interactions with Asn101 were observed for both models (Tables 2 and 3). In LacY based model all ligands except for (3) and (5) interacted with Asn101, while in $LeuT_{Aa}$ based SERT model compounds (**1**), (**4**) and (**6**) were in close contact with this amino acid. Ligand interactions with Gly100 in TMH1 were observed only for the $LeuT_{Aa}$ based SERT model (Tables 2 and 3).

Experimental studies also indicated that a close location of TMH1 and TMH3 is necessary for proper ligand recognition and binding to SERT.[25] In both of SERT models TMH1 and TMH3 were located in close connection to each other, while direct interactions between ligands and amino acids in TMH3 were seen only for the $LeuT_{Aa}$ based SERT model (Table 3). The residues in TMH3 involved in ligand binding to $LeuT_{Aa}$ based SERT model were (Table 3): Ala169, Ile172, Ala173, Tyr175 and Tyr176. These results are in agreement with experimental studies revealing that Ile172 and Tyr176 in TMH3 are in close proximity to the binding site for 5-HT and cocaine.[35]

In the $LeuT_{Aa}$ based SERT model, but not in the LacY based SERT model amino acids in TMH6 were involved in ligand binding (Tables 2 and 3). In the model based on the $LeuT_{Aa}$ structure, the piperazine ring of the ligands was in contact with the aromatic rings of Tyr176 (TMH3) and Phe335 (TMH6). The interactions between the methyl group at the piperazine ring of compounds (**1**)–(**4**) and the aromatic ring of Phe335 seemed to stabilize the complex, and may explain why the methylated compounds interact stronger with SERT than did the compounds without the methyl group (Table 1). In the $LeuT_{Aa}$ based SERT model the side chains of Arg104 (TMH1), Tyr175 (TMH3) and Thr497 (TMH10) were facing the quinoline moiety of the ligands while the ligands imide moiety was in contact with Tyr95 in TMH1, Phe341 in TMH6 and Ser438 and Gly442 in TMH8.

A previous molecular modelling study using $LeuT_{Aa}$ as a template suggested that after binding of 5-HT to the human SERT, Tyr176 (TMH3) forms a hydrogen bond with Asp98 (TMH1), whereas after binding of escitalopram Tyr176 (TMH3) is in contact with Ser438 (TMH8).[34] A close interaction between Tyr176 (TMH3) and Ser438 (TMH8) was also observed after docking of the buspirone analogues to the $LeuT_{Aa}$ based SERT model, indicating similarities in the binding of known SSRIs and the compounds in the present study. The observed differences in side chain packing between substrate and inhibitor bound states[24] may indicate that the ligands may bind SERT by an induced fit mechanism.[36,37] An induced fit mechanism has been also proposed for LacY to explain the mechanism of coupling between lactose and H+ translocation.[38] For compounds (**1**)–(**4**) with quite high affinity for SERT (Table 1), close interactions between the imide moiety of the ligands and Tyr95 (TMH1) and Ser438 (TMH8) were observed. These interactions seemed to stabilize the ligand–SERT complex. The imide moiety of compounds (**5**)–(**7**) was located approximately 4–5 Å from these residues. These differences in the interactions of the imide moiety with Tyr95 and Ser438 may explain why compounds (**1**)–(**4**) have higher affinity for SERT than compounds (**5**)–(**7**).

Site-directed mutagenesis studies of DAT indicated that amino acids in TMH4 (Tyr267, SERT numbering)[39], TMH5 (Tyr289, SERT numbering)[27] and TMH11 (Phe551, Phe556, SERT numbering)[39] are important for cocaine binding and substrate translocation. These observations are in agreement with the SERT model based on LacY (Table 2), but not with the model based on the $LeuT_{Aa}$ crystal structure (Table 3). However, it has been suggested based on accessibility studies of SERT that TMH5 might contribute to the substrate-permeation pathway on the cytoplasmic side.[40] The $LeuT_{Aa}$ based SERT model is closed at the cytoplasmic side, while during substrate translocation this side is more open such that TMH5 may be accessible from the cytoplasmic side.

Experimental studies also provided support for involvement of TMH7 in SERT substrate recognition and transport.[25,41] Although TMH7 is in close proximity to the substrate translocation area in both SERT models, the studied buspirone analogues were in direct contact (van der Waals contacts) with amino acids in TMH7 only in LacY based SERT model (Tables 2 and 3). Interactions between amino acids in TMH2 and ligands were observed only for the LacY based SERT model. Furthermore, in both SERT models the TMH10 was involved in ligand binding. Experimental accessibility studies of SERT indicate that TMH10 might participate in the transition to a cytoplasmic facing conformation of SERT.[40]

Recent data on binding of the tricyclic antidepressants (TCA) such as clomipramine[42] and desipramine[49] to the $LeuT_{Aa}$ transporter proteins show that these compounds bind to $LeuT_{Aa}$ in the extracellular-facing vestibule that probably forms part of permeation pathway, lying between the extracellular solution and the occluded substrate- and ion-binding pocket located halfway across the membrane bilayer. By stabilizing the extracellular gate in closed conformation clomipramine/desipramine noncompetitively inhibits the substrate uptake of $LeuT_{Aa}$. In the SERT model based on the $LeuT_{Aa}$ crystal structure a putative substrate-binding site corresponding to the leucine-binding site of $LeuT_{Aa}$ was formed by a pore between TMHs 1, 3, 6, 8 and 10 (Table 3). Inhibitor dissociation experiments using tricyclic antidepressant unveiled the existence of a low-affinity binding site on SERT that was shown to slow the dissociation of inhibitors from a high-affinity binding site.[43] The ICM Pocket Finder identified a second putative-binding site at the $LeuT_A$ based model, but not at the LacY based model. This binding site constituted amino acids in TMH1, TMH6, TMH10 and TMH11 (Table 4). The amino acids in TMH1, TMH6 and TMH10 are well conserved between $LeuT_{Aa}$ and SERT, while the amino acids in TMH11 involved in the binding site are less conserved (Table 1). The buspirone analogues were also docked into this binding site, and calculations of the molecular interactions energies between the compounds and SERT indicated that this binding region may correspond to the low-affinity binding site. In this binding site the compounds were bound in extracellular-facing cavity containing of the transmembrane helices TMH1, TMH6, TMH10, TMH11 and extracellular loop EL4, similar to clomipramine/desipramine in the $LeuT_{Aa}$ structure.[42,49] Clomipramine in complex with $LeuT_{Aa}$ is stabilized by a salt bridge between its protonated nitrogen atom and Asp401, and by polar interactions of its chlorine atom with Gln34 in the binding site. Desipramine probably also forms a salt bridge with an aspartate residue.[49] The residues Lys490 and Ile108 in SERT correspond to Asp401 and Gln34 in $LeuT_{Aa}$, respectively, were located in close proximity to the buspirone analogues in the low-affinity binding site. However, in the complexes of the buspirone analogues with SERT the protonated nitrogen atom at piperazine ring was close to Asp328 in TMH6. The clomipramine/desipramine-$LeuT_{Aa}$ complex indicated that these tricyclic compounds probably are retarding the unbinding of the substrate through the extracellular pathway by stabilizing the salt bridge between Asp404 and Arg30. The residues Glu493 and Arg104 in SERT correspond to Asp404 and Arg30 in $LeuT_{Aa,}$ and were close to the ligands in both the putative low-affinity binding site and the putative high-affinity binding site which correspond to the leucine-binding site in $LeuT_{Aa}$. In the desipramine-$LeuT_{Aa}$ complex, it was shown that the desipramine-binding site and leucine-binding site are nonoverlapping but they share Phe253 as a common residue (corresponding to Phe335 in SERT).[49] Thus, it can be suggested that high- and low-affinity binding site in SERT do not overlap each other, but they share residues such as Arg104 and Glu493.

It was suggested that movements of the extracellular loop EL4 participated in TCA binding of $LeuT_{Aa}$.[42,49] EL4 in SERT is connecting TMH7 and TMH8, has been hypothesized to play a role in conformational changes associated with substrate translocation.[44] The amino acid residue Gly402 in EL4 of SERT corresponding to Ala321 in $LeuT_{Aa}$ was involved in binding of the buspirone analogues to the low-affinity binding site. Ligand binding to the low-affinity binding site might prevent the extracellular-facing cavity from compacting during interconversion to an intracellular-facing form. Such a condensation in the extracellular-facing form has been postulated to occur in SERT,[40,44] where the extracellular inhibitor cocaine is though to prevent such a compaction from occurring to preclude subsequent opening of the cytoplasmic permeation pathway. Moreover, mutagenesis experiments on SERT and DAT indicate that both the desipramine-binding site and its inhibition mechanism most probably are conserved amongst human neurotransmitter transporters.[49]

4. Conclusions

In the present study we have used the X-ray structures of LacY and $LeuT_{Aa}$ to construct models of SERT. $LeuT_{Aa}$ is much more similar to SERT both in sequence and function and are believed to be a more suitable template for SERT modelling than LacY. The docking of buspirone analogues into the SERT models indicated differences in ligand recognition. Both the LacY based SERT model and the $LeuT_{Aa}$ based SERT model confirmed results of site-directed mutagenesis studies, but neither of the models could account for all residues known to be important for ligand binding. Docking studies indicated that experimental results that could not be explained by the structure of the $LeuT_{Aa}$ based model, was explained by the LacY based model.

Substrate translocation and ligand binding induce large conformational changes. The reaction cycle of the secondary transporters might involve at least three states: open to outside, occluded, and open to the inside. Although the conformations of the SERT model based on the LacY structure after MD simulations were different from that in the $LeuT_{Aa}$ based SERT model it can not be completely ruled out that that they represent different energetically favourable conformations of the same folding class. Thus, different inhibitors may bind to different conformational stages of SERT. Residues involved in ligand binding were identified, whereas further studies of ligand binding to different conformations of SERT are essential to obtain models of value for virtual screening and target-based ligand design. The docking of ligands to a binding site which might correspond to a low-affinity binding site pinpointed an additional region that might be considered for development new inhibitors.

5. Methods

5.1. 5-HTT-binding experiments

The affinity of the analyzed compounds for SERT in vitro was carried out on isolated rat synaptosomes, according to the method of Owens et al.[50] with slight modifications. The rat cerebral cortex was homogenized in 30 volumes of ice-cold Tris–HCl buffer (50 mM, pH 7.7 at 25 °C) containing 150 mM NaCl and 5 mM KCl. Then the homogenate was centrifuged at 20,000*g* for 20 min. The supernatant was decanted and pellet was resuspended in 30 volumes of buffer and centrifuged again. The resulting pellet was resuspended in the same quantity of the buffer and centrifuged third time in the same conditions. [^{3}H]Citalopram (specific activity 50 Ci/mmol, NEN Chemicals) was used for labelling 5-HT transporter. The tissue homogenate (240 μl) with 30 μl of 1 μM imipramine (displacer), 30 μl of 1 nM [^{3}H]citalopram and 100 μl of the analyzed compound was incubated for 1 h at 22 °C. The concentrations of analyzed compounds ranged from 10^{-10} to 10^{-4} M. Incubations were terminated by vacuum filtration over Whatman GF/B glass fibre filters, and washed two times with 100 μl of ice-cold buffer. Radioactivity was measured in WALLAC 1409 DSA liquid scintillation counter. All assays were done in duplicates. Radioligand-binding data were analyzed using iterative curve fitting routines (GraphPAD/Prism, version 3.0-San Diego, CA, USA).

5.2. Molecular modelling

5.2.1. The SERT models

5.2.1.1. The SERT models based on the LacY template. An initial model of the helical bundle was constructed based on the crystal structure of LacY from *E. coli*[13] (PDB-id: 1PV6) using the

traditional homology modelling approach as implemented in the ICM program.[20] The alignment used for the modelling is shown in Figure 1. The amino acid sequence of the human serotonin transporter (hSERT)[51] was obtained from the Swiss Prot database (http://www.expasy.ch/sprot/; P31645). The fast routine for building a complete model by homology with loops combined with the database search for the best conformation of the loops was carried out with procedure described by Ravna et al.[15] The N- and C-terminal structures were taken directly from a previous SERT model.[52]

The LacY structure used as a template for the SERT modelling represented an inward-facing conformation. In the inward-facing conformation the central hydrophilic cavity containing the sugar-binding site is open towards the cytoplasmic site. Our intention was to study ligand interactions, and an outward-facing conformation open to the periplasmic side was therefore constructed. Abramson et al.[13] suggested a model for the structural changes into an outward-facing LacY conformation. Using their description as a guideline, a rigid-body rotation of ~60° between the N- and C-terminal domains of the inward-facing conformation around an axis perpendicular to membrane was used to generate an outward-facing SERT model. Figure 2 is showing both the inward- and outward-facing SERT models constructed by homology with LacY. The outward-facing SERT model was used for ligand docking and for molecular dynamics simulations (MD) of SERT–ligand complexes. However, in contrast to previous studies,[15] the N- and C-terminal and the loops between helices were removed from the SERT model used for ligand docking and MM and MD calculations. Information about familiar conversation and the results of site-directed mutagenesis studies of neurotransmitter transporters (SERT, DAT and NET) were used to define the start and end points of the 12 TMHs. To protect the helical ends during calculations, two protecting groups: ACE (acetyl beginning group) and NME (amine ending group), were added using Xleap program implemented in Amber 8.0.[53]

5.2.1.2. The SERT model based on the $LeuT_{Aa}$ template. The leucine transporter ($LeuT_{Aa}$) (PDB-id: 2a65) is a bacterial homologue of SERT, and the X-ray structure provided the opportunity to construct a new and most probably more correct 3D model of SERT.[14,16] The crystallization captured the $LeuT_{Aa}$ protein in a state with the substrate leucine bound at the active site, and both the extracellular and intracellular gates closed. Therefore, the SERT model build by homology with $LeuT_{Aa}$ (Fig. 1) may correspond to a substrate-bound conformation of SERT, closed at both sites of the membrane (Fig. 3). The loops and C- and N-terminal domains were present in the second SERT model during calculations. The model was used for docking of buspirone analogues.

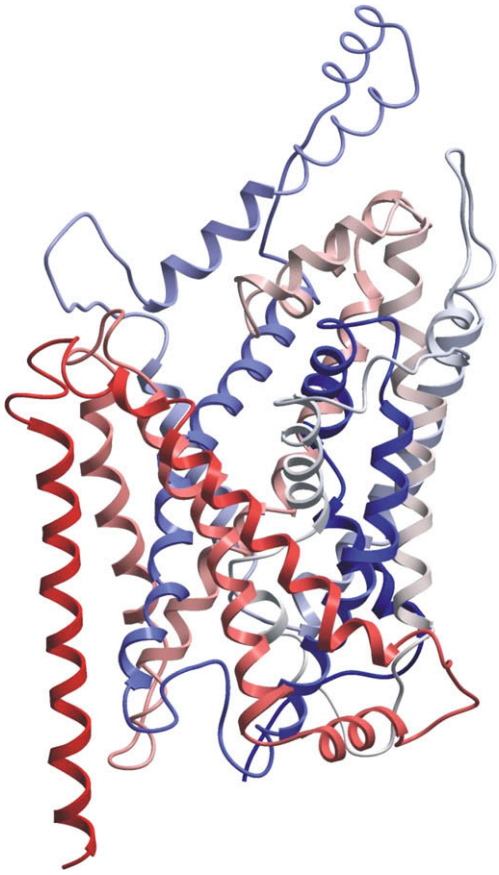

Figure 3. The SERT model based on the X-ray crystal structure of the $LeuT_{Aa}$ transporter from *Aquifex aeolicus*. The model is coloured from amino (red) to carboxy (blue) terminal.

5.2.2. Modelling of ligands

The serotonin molecule and starting geometries of the ligands (**1**–**3** and **7**) (Table 1) were built using the Xleap program implemented in Amber 8.0.[53] The initial structures of ligands (**4**–**6**) (Table 1) were taken from previous studies.[54,55] The nitrogen atom attached to the butyl fragment was protonated in all ligands. After

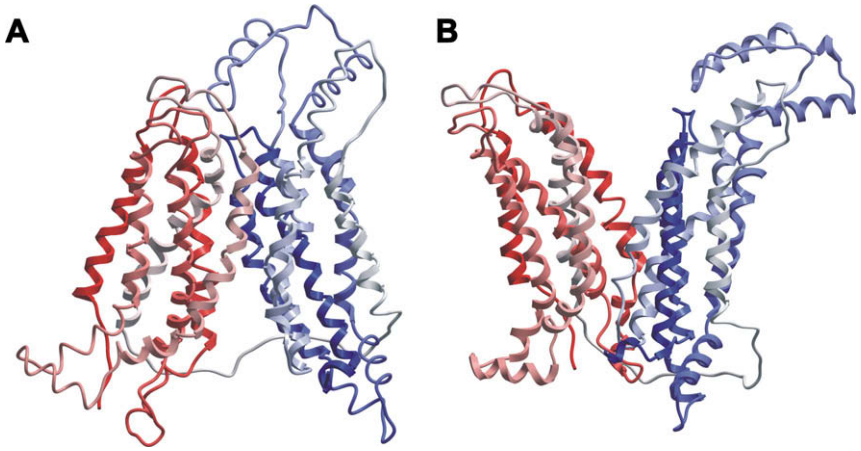

Figure 2. SERT models based on the X-ray crystal structure of the LacY transporter from *Escherichia coli*. (A) Inward-facing conformation. (B) Outward-facing conformation. The models are coloured from amino (red) to carboxy (blue) terminal.

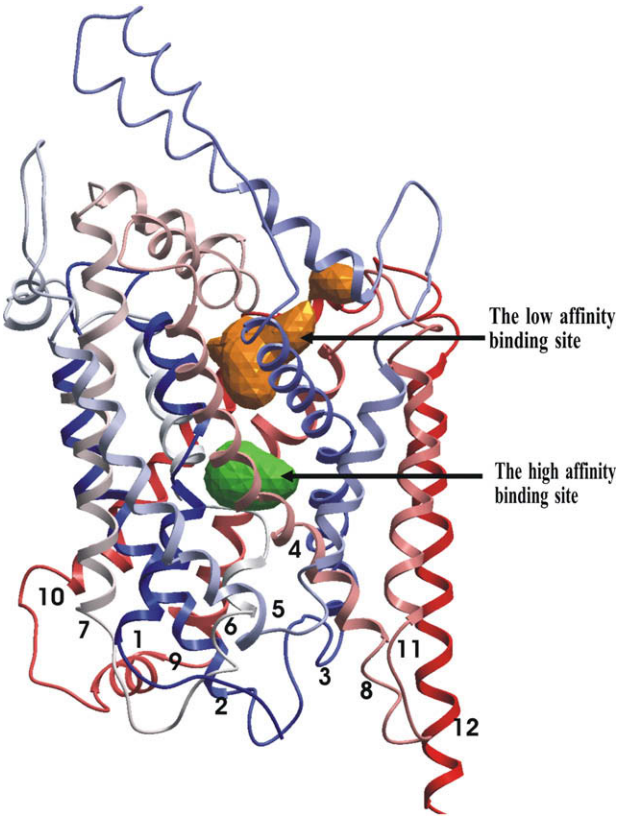

Figure 4. Putative pockets for high- and low-affinity ligand binding to the SERT model based on $LeuT_{Aa}$ crystal structure (coloured red and blue, respectively). The cytoplasmic side is up in the figure.

interactive docking into the SERT model based on LacY, the geometry of the ligands were optimized, and atomic point charges were calculated using an RHF/6-31G* basis set and RESP fitting by the Gaussian98 program.[56] The major strength of the RESP charges is that they optimally reproduce the intermolecular interaction properties of molecules with a simple two-body additive potential.

5.2.3. Ligand docking

5.2.3.1. Docking into the LacY based SERT model. Serotonin was docked into the LacY based SERT model both in the inward- and outward-facing conformation. The buspirone analogues (Table 1) were docked into the outward-facing SERT model (Fig. 5A) using a flexible Monte Carlo docking procedure as implemented in the ICM software.[20] The binding site constituted amino acids mainly in TMH1, TMH2, TMH4, TMH5, TMH7, TMH8 and TMH10 (Fig. 6). The functional important residue for ligand anchoring was Asp98 in TMH1.[57] The ligand molecules were fully flexible and the protein was represented by grid interaction potentials. Geometrically different low-energy conformations of the ligands from the ligand–SERT complexes were accumulated in a conformational stack.

5.2.3.2. Docking into the $LeuT_{Aa}$ based SERT model. The buspirone analogues were also docked into the $LeuT_{Aa}$ based SERT model. The ICMPocketFinder indicated a possible binding pocket in the $LeuT_{Aa}$ based model in the area corresponding to the leucine-binding site of $LeuT_{Aa}$, and corresponding to the docking site of the LacY based model (Fig. 5B). This binding site constituted mainly amino acids in TMH1, TMH3, TMH6, TMH8 and TMH10 (Fig. 6). Asp98 in TMH1 was also the anchoring point for the docking into this model. The binding site constitutes several amino acids found to be important for ligand binding, and most probably may correspond to the suggested high-affinity binding site.[57,58]

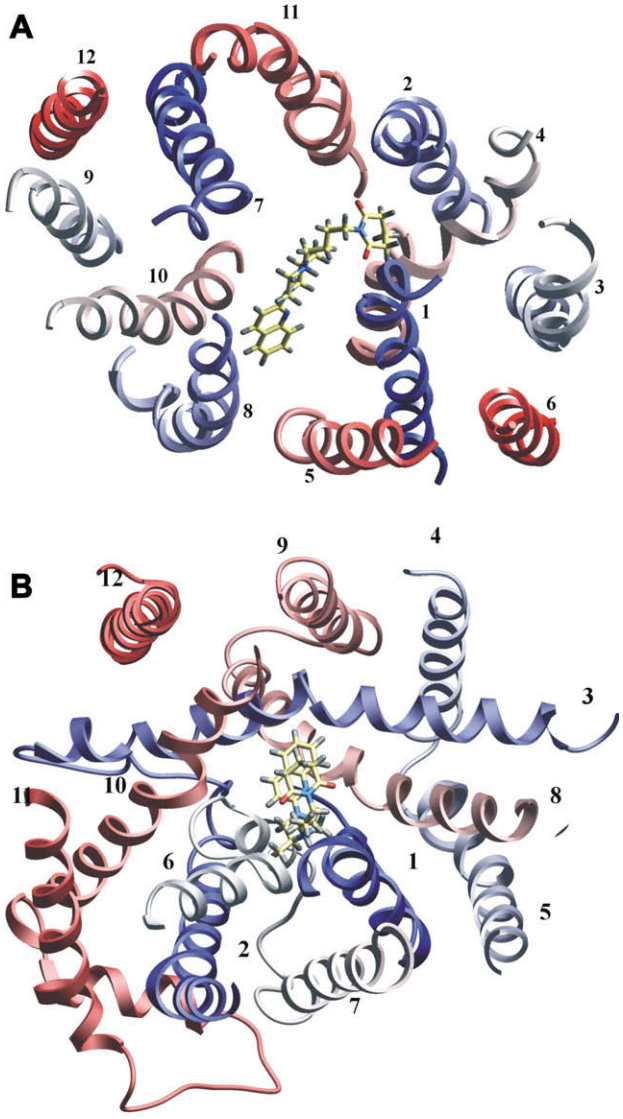

Figure 5. The binding sites of the buspirone analogues in the models based on: (A) the crystal structure of LacY from *Escherichia coli* in the outward-facing conformation and (B) the crystal structure of the $LeuT_{Aa}$ transporter from *Aquifex aeolicus*.

The ICMPocketFinder also identified a putative second-binding site that might correspond the suggested low-affinity binding site[59,60] on SERT. This binding site includes residues from TMH1, TMH6, TMH10 and TMH11 (Fig. 8). Asp328 was used as the ligand anchoring in the docking procedure. As shown at Figure 4 the putative high-affinity binding pocket is located deeper within the protein core than the putative pocket for low-affinity binding, which is located in extracellular-facing cavity of SERT.

The ligands were docked into the two possible binding sites using the automatic docking module of the ICM molecular modelling software and a procedure similar to the docking into the LacY based SERT model.

5.2.4. The serotonin transporter–ligand complex modelling

5.2.4.1. The SERT model based on the LacY structure. MD simulations of complexes with the SERT model based on the LacY template were performed in order to study if the helical architecture could change into a more similar to that of the $LeuT_{Aa}$ based SERT model. Conformational changes of SERT are required during substrate binding and translocation. In order to get an insight into

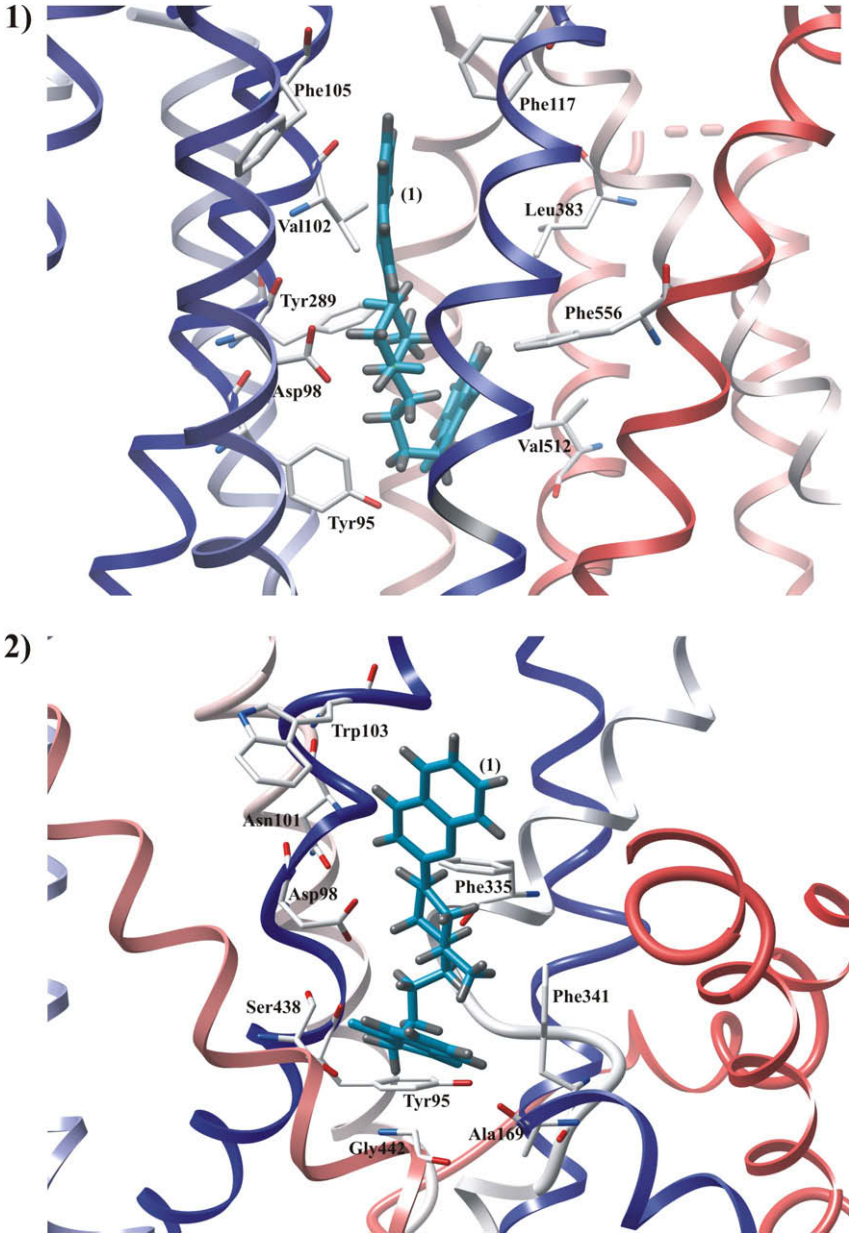

Figure 6. The most important amino acids for binding of buspirone analogues (ligand (1) as an example) are indicated for the SERT model based on: (1) the crystal structure of LacY from *Escherichia coli* and (2) the crystal structure of $LeuT_{Aa}$ from *Aquifex aeolicus*.

substrate transport mechanisms, the complexes of serotonin bound to the SERT model both in the inward- and outward-facing conformation were analyzed. After docking of buspirone analogues into the outward-facing conformation, the lowest-energy complex of each ligand with SERT was selected and used as starting complexes of molecular mechanics energy minimisations (MM) and molecular dynamics (MD) simulations with Amber 8.0 using the Cornell force field.[61] MM and MD calculations were performed for the LacY based SERT model only. In order to preserve the helical conformation of the helical bundle, extra forces were applied to intrahelical hydrogen bonds, between the backbone oxygen atom of residue n and the hydrogen atom connected to backbone nitrogen atom of residue $n+4$, excluding prolines. The effective force constant was multiplied by the weight of the restraints. During MM restraints with a weight of 1.0 kcal/mol Å were restraining the helical transmembrane part of the SERT model. MMs were performed by 500 steps of steepest descent minimisation followed by 2000 steps of conjugate gradient minimisation until convergence. The convergence criteria were 0.02 kcal/mol Å RMS differences for the norm of the energy gradient between successive steps and the cut off radius for non-bonded interactions was 15 Å. The minimised structures of SERT–ligand complexes were used as initial structures for MD simulations. During MD calculations the weight of restrains was gradually increased from 0.1 to 1.0 kcal/mol Å between 0 and 50 ps and was kept at 1.0 kcal/mol Å for the rest of the run (from 50 to 130 ps). Starting with a smaller weight on the restraints ensures that the structure will quickly adjust to overcome bad conformations. MD was performed with a cut off radius for non-bonded interactions at 12 Å, and a secondary cut off radius of 15 Å.

The protocol for the simulation was as follows:

1. 0–30 ps heating of the complexes. The temperature was gradually increased from 0 to 300 K (an increase of 50 K each 1 ps MD).
2. 30–80 ps, equilibration at 300 K.

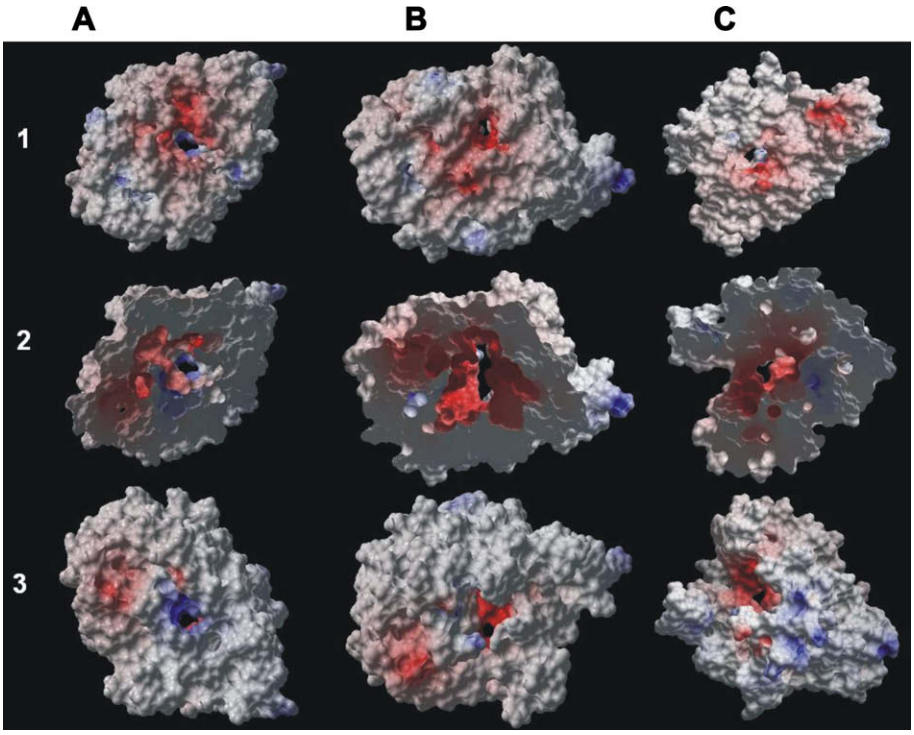

Figure 7. The serotonin transporter potential energy surface for: (A) an inward-facing conformation. (B) An outward-facing conformation of the SERT model based on the X-ray crystal structure of LacY and (C) for the SERT model based on the X-ray crystal structure of $LeuT_{Aa}$. (1) The electrostatic potential distribution viewed from the periplasmic side. (2) The electrostatic potential distribution viewed in the middle of the membrane. (3) The electrostatic potential distribution viewed from the cytoplasmic side. The most negative electrostatic potentials are colored red, while the most positive electrostatic potentials are colored blue.

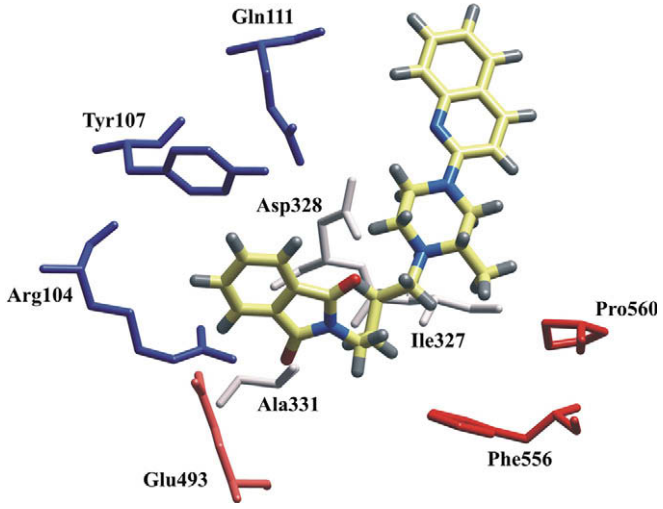

Figure 8. The putative low-affinity binding site in the SERT model based on the crystal structure of the $LeuT_{Aa}$ transporter from *Aquifex aeolicus*. The residues having van der Waals contacts with ligands are shown.

3. 80–130 ps of MD at 300 K with sampling of coordinates every 1 ps.

The average structure of each SERT–ligand complex from the MD sampling period was obtained using the Carnal module of the Amber package[53] and energy minimised. The complexes were analyzed using Carnal module, and amino acid residues involved in ligand binding were identified.

5.2.4.2. The SERT model based on the $LeuT_{Aa}$ structure. The buspirone analogues were also docked into the $LeuT_{Aa}$ based SERT model. For each ligand, about 40 SERT–ligand complexes were examined. For each ligand, the best pose was selected based on the scoring functions implemented in the ICM program[20] and Xscore program,[62] and by visual inspection of the interactions with amino acid residues inside the binding pocket. The selected ligand–SERT complexes were energy minimized with the Amber 8.0[53] using the same procedure as for the complexes of the LacY based SERT model with ligands. MD calculations were not performed for complexes of the $LeuT_{Aa}$ based SERT model.

Acknowledgements

This work was financially supported by KBN Grant No. 3 T09A 032 29. Authors thank for the support of the Norwegian Research Council, and by computer time on the HP supercomputer at the University of Tromsø.

References and notes

1. Vaswani, M.; Linda, F. K.; Ramesh, S. *Prog. Neuropsychopharmacol.* **2003**, *271*, 85.
2. Jones, B. J.; Blackburn, T. P. *Pharmacol. Biochem. Behav.* **2002**, *71*, 555.
3. Blier, P.; de Montigny, C. *Trends Pharmacol. Sci.* **1994**, *15*, 220.
4. Artigas, F.; Romero, L.; de Montigny, C.; Blier, P. *Trends Neurosci.* **1996**, *19*, 378.
5. Hjorth, S. *J. Neurochem.* **1993**, *60*, 776.
6. Dreshfield, L. J.; Wong, D. T.; Perry, K. W.; Engleman, E. A. *Neurochem. Res.* **1996**, *21*, 557.
7. Takeuchi, K.; Kohn, T. J.; Honigschmidt, N. A.; Rocco, V. P.; Spinazze, P. G.; Atkinson, S. T.; Hertel, L. W.; Nelson, D. L.; Wainscott, D. B.; Ahmad, L. J.; Shaw, J.; Threlkeld, P. G.; Wong, D. T. *Bioorg. Med. Chem. Lett.* **2003**, *13*, 1903.
8. Takeuchi, K.; Kohn, T. J.; Honigschmidt, N. A.; Rocco, V. P.; Spinazze, P. G.; Atkinson, S. T.; Hertel, L. W.; Nelson, D. L.; Wainscott, D. B.; Ahmad, L. J.; Shaw, J.; Threlkeld, P. G.; Wong, D. T. *Bioorg. Med. Chem. Lett.* **2003**, *13*, 2393.
9. Takeuchi, K.; Kohn, T. J.; Honigschmidt, N. A.; Rocco, V. P.; Spinazze, P. G.; Atkinson, S. T.; Hertel, L. W.; Nelson, D. L.; Wainscott, D. B.; Ahmad, L. J.; Shaw, J.; Threlkeld, P. G.; Wong, D. T. *Bioorg. Med. Chem. Lett.* **2003**, *13*, 3939.
10. Saier, M. H. *Microbiology* **2000**, *146*, 1775.
11. Yin, Y.; He, X.; Szewczyk, P.; Nguyen, T.; Chang, G. *Science* **2006**, *312*, 741.
12. Huang, Y.; Lemieux, M. J.; Song, J.; Auer, M.; Wang, D. N. *Science* **2006**, *30*, 616.

13. Abramson, J.; Smirnova, I.; Kasho, V.; Verner, G.; Kaback, H. R.; Iwata, S. *Science* **2003**, *301*, 616.
14. Yamashita, A.; Singh, S. K.; Kawate, T.; Jin, Y.; Gouaux, E. *Nature* **2005**, *437*, 215.
15. Ravna, A. W.; Sylte, I.; Kristiansen, K.; Dahl, S. G. *Bioorg. Med. Chem.* **2006**, *14*, 666.
16. Ravna, A. W.; Jarończyk, M.; Sylte, I. *Bioorg. Med. Chem. Lett.* **2006**, *16*, 5594.
17. Krajewski, J. K. Ph.D. thesis, Warsaw, 2001.
18. Chilmonczyk, Z.; Cybulski, M.; Iskra-Jopa, J.; Chojnacka-Wójcik, E.; Taterczyńska, E.; Kłodzińska, A.; Leś, A.; Bronowska, A.; Sylte, I. *Farmaco* **2002**, *57*, 285.
19. Krajewski, J. K.; Leś, A.; Cybulski, M.; Chilmonczyk, Z.; Bronowska, A.; Szelejewska-Woźniakowska, A. *Pol. J. Chem.* **2001**, *75*, 71.
20. Abagyan, R.; Totrov, M.; Kuznetsow, D. N. *J. Comput. Chem.* **1994**, *15*, 488.
21. Henry, L. K.; DeFelice, L. J.; Blakely, R. D. *Neuron* **2006**, *49*, 791.
22. Beuming, T.; Javitch, J. A.; Weinstein, H. *Mol. Pharmacol.* **2006**, *70*, 1630.
23. Jørgensen, A. M.; Tagmose, L.; Jørgensen, A. M. M.; Topiol, S.; Sabio, M.; Gundertofte, K.; Bøgesø, K. P.; Peters, G. H. *ChemMedChem* **2007**, *2*, 815.
24. Jørgensen, A. M.; Tagmose, L.; Jørgensen, A. M. M.; Bøgesø, K. P.; Peters, G. H. *ChemMedChem* **2007**, *2*, 827.
25. Henry, L. K.; Field, J. R.; Adkins, E. M.; Parnas, M. L.; Vaughan, R. A.; Zou, M.; Newman, A. H.; Blakely, R. D. *J. Biol. Chem.* **2006**, *281*, 2012.
26. Barker, E. L.; Perlman, M. A.; Adkins, E. M.; Houlihan, W. J.; Pristupa, Z. B.; Niznik, H. B.; Blakely, R. D. *J. Biol. Chem.* **1998**, *273*, 19459.
27. Kitayama, S.; Shimada, S.; Xu, H.; Markham, L.; Donovan, D. M.; Uhl, G. R. *Proc. Natl. Acad. Sci. U.S.A.* **1992**, *89*, 7782.
28. Lin, Z.; Wang, W.; Kopajtic, T.; Revay, R. S.; Uhl, G. R. *Mol. Pharmacol.* **1999**, *56*, 434.
29. Lee, S. H.; Chang, M. Y.; Lee, K. H.; Park, B. S.; Lee, Y. S.; Chin, H. R. *Mol. Pharmacol.* **2000**, *57*, 883.
30. Larsen, M. B.; Elfving, B.; Wiborg, O. *J. Biol. Chem.* **2004**, *279*, 42147.
31. Mortensen, O. V.; Kristensen, A. S.; Wiborg, O. *J. Neurochem.* **2001**, *79*, 237.
32. Roubert, C.; Cox, P. J.; Bruss, M.; Hamon, M.; Bonisch, H.; Giros, B. *J. Biol. Chem.* **2001**, *276*, 8254.
33. Lin, Z.; Wang, W.; Uhl, G. R. *Mol. Pharmacol.* **2000**, *58*, 1581.
34. Henry, L. K.; Adkins, E. M.; Han, Q.; Blakely, R. D. *J. Biol. Chem.* **2003**, *278*, 37052.
35. Chen, J.-G.; Sachpatzidis, A.; Rudnick, G. *J. Biol. Chem.* **1997**, *272*, 28321.
36. Koshland, D. E., Jr. *Proc. Natl. Acad. Sci. U.S.A.* **1958**, *44*, 98.
37. McCammon, J. A. *Curr. Opin. Struct. Biol.* **1998**, *8*, 245.
38. Mirza, O.; Guan, L.; Verner, G.; Iwata, S.; Kaback, H. R. *EMBO J.* **2006**, *25*(6), 1177.
39. Kitayama, S.; Morita, K.; Dohi, T.; Wang, J. B.; Davis, S. C.; Uhl, G. R. *Ann. N.Y. Acad. Sci.* **1996**, *801*, 388.
40. Zhang, Y.-W.; Rudnick, G. *J. Biol. Chem.* **2006**, *281*, 36213.
41. Kamdar, G.; Penado, K. M.; Rudnick, G.; Spethan, M. M. *J. Biol. Chem.* **2001**, *276*, 4038.
42. Singh, S. K.; Yamashita, A.; Gouaux, E. *Nature* **2007**, *448*, 952.
43. Neubauer, H. A.; Hansen, C. G.; Wiborg, O. *Mol. Pharmacol.* **2006**, *69*, 1242.
44. Mitchell, S. M.; Mayra, E. L.; Garcia, L.; Stephan, M. M. *J. Biol. Chem.* **2004**, *279*, 24089.
45. Akabas, M.; Stauffer, D.; Karlin, M.; Xu, A. *Science* **1992**, *8*, 307.
46. Javitch, J.; Li, X.; Kaback, J.; Karlin, A. *Proc. Natl. Acad. Sci. U.S.A.* **1994**, *91*, 10355.
47. Holmgren, M.; Liu, Y.; Xu, Y.; Yellen, G. *Neuropharmacology* **1996**, *35*, 797.
48. Chen, J. G.; Liu-Chen, S.; Rudnick, G. *Biochemistry* **1997**, *36*, 1479.
49. Zhou, Z.; Zhen, J.; Karpowich, N. K.; Goetz, R. M.; Law, C. J.; Reith, M. E. A.; Wang, D.-N. *Science* **2007**, *317*, 1390.
50. Owens, M. J.; Morgan, W. N.; Plott, S. J.; Nemeroff, C. B. *J. Pharmacol. Exp. Ther.* **1997**, *283*, 1305.
51. Ramamoorthy, S.; Bauman, A. L.; Moore, K. R.; Han, H.; Yang-Feng, T.; Chang, A. S.; Ganapathy, V.; Blakely, R. D. *Proc. Natl. Acad. Sci. U.S.A.* **1993**, *90*, 2542.
52. Ravna, A. W.; Sylte, I.; Dahl, S. G. *J. Pharmacol. Exp. Ther.* **2004**, *307*, 34.
53. Case, D. A.; Darden, T. A.; Cheatham, T. E.; Simmerling, C. L., III; Wang, J.; Duke, R. E.; Luo, R.; Merz, K. M.; Wang, B.; Pearlman, D. A.; Crowley, M.; Brozell, S.; Tsui, V.; Gohlke, H.; Mongan, J.; Hornak, V.; Cui, G.; Beroza, P.; Schafmeister, C.; Caldwell, J. W.; Ross, W. S.; Kollman P. A. AMBER 8, University of California, San Francisco, 2004.
54. Bronowska, A.; Leś, A.; Chilmonczyk, Z.; Filipek, S.; Edvardsen, Ø.; Østensen, R. *Bioorg. Med. Chem.* **2001**, *9*, 881.
55. Bronowska, A.; Chilmonczyk, Z.; Leś, A.; Edvardsen, Ø.; Østensen, R.; Sylte, I. *J. Comput. Aided Mol. Des.* **2001**, *15*, 1005.
56. Bayly, C. I.; Cieplak, P.; Cornell, W. D.; Kollmann, P. A. *Phys. Chem.* **1993**, *97*, 10269.
57. Barker, E. L.; Moore, K. R.; Rakhshan, F.; Blakely, R. D. *J. Neurosci.* **1999**, *19*, 4705.
58. Adkins, E. M.; Barker, E. L.; Blakely, R. D. *Mol. Pharmacol.* **2001**, *59*, 514.
59. Plenge, P.; Wiborg, O. *Neurosci. Lett.* **2005**, *383*, 203.
60. Chen, F.; Larsen, M. B.; Neubauer, H. A.; Sánchez, C.; Plenge, P.; Wiborg, O. *J. Neurochem.* **2005**, *92*, 21.
61. Cornell, W. D.; Cieplak, P.; Bayly, C. I.; Gould, I. R.; Merz, K. M.; Ferguson, D. M.; Spellmeyer, D. C.; Fox, T.; Cadlwell, J. W.; Kollmann, P. A. *J. Am. Chem. Soc.* **1995**, *117*, 5179.
62. Wang, R.; Lai, L.; Wang, S. *J. Comput. Aided Mol. Des.* **2002**, *16*, 11 [X-Score].